

Research Note

Electron densities in EUV coronal bright points

I. Ugarte-Urra¹, J. G. Doyle¹, and G. Del Zanna²

¹ Armagh Observatory, College Hill, Armagh BT61 9DG, N. Ireland

² Mullard Space Science Laboratory, Holmbury St. Mary, Dorking, Surrey RH5 6NT, UK

Received / Accepted

Abstract. Electron density measurements of six coronal bright points have been obtained using line ratio diagnostics of four ions in the temperature range $1.3\text{--}2.0\times 10^6$ K. The results suggest that BP plasma has more similarities to active region plasma than to quiet Sun plasma. Nevertheless, they do not show the exact same behaviour: the increase of electron density at temperatures over $\log T_e \sim 6.2$, observed in the core of active regions, has not been detected. The Fe xii results based on new atomic data, although in better agreement decreasing more than a factor of two the densities obtained with older calculations, are still in some instances higher than those from Si x. This could be a consequence of the inhomogeneity of the plasma in the observed volume. New measurements with a better constriction of the volumetric properties seem necessary to rule out the influence of other factors and confirm whether there is an inconsistency between the ions, perhaps due to line blending problems in the Fe xii lines.

Key words. Sun: corona – Sun: fundamental parameters – Hydrodynamics

1. Introduction

Determining properties like the electron density, temperature, pressure or the speed of possible flows present in coronal structure, is crucial in order to characterize the existing plasma and understand which are the possible mechanisms that can heat it. The identification of the dominant heating mechanism will take place when the appropriate coronal model is able to reproduce all these observables at any given condition. The electron density is a key parameter in these studies as atomic processes dominate the population and depopulation of the atomic levels and the transitions that originate from them. Therefore it plays an important role in the determination of the radiative losses in the coronal heating models.

So far, to our knowledge, there has been no spectroscopic study of electron densities in EUV coronal bright points (hereafter BPs), apart from certain isolated values (Del Zanna et al. 2003). Therefore, as part of a larger spectroscopic study of their properties (Ugarte-Urra et al. 2004a,b; Ugarte-Urra 2004), we present, and place in context, electron densities for several BPs derived from density sensitive line ratios. BPs are small regions ($\lesssim 30$ Mm) of enhanced EUV emission over the surrounding corona, associated to the interaction of opposite bipolar magnetic features. Their lifetimes are in the range 1–60 hours (McIntosh & Gurman 2004).

2. Observations

Six different coronal bright points were observed with the Coronal Diagnostic Spectrometer CDS/SOHO between the 31st July and the 5th August 1997, during a period of minimum solar activity when BPs are more clearly identified in the solar disk due to the absence of active regions. The CDS Normal Incidence Spectrometer (NIS) rastered $122''\times 119''$ areas of the Sun by taking sixty 50 second exposures at adjacent solar X positions using the $2''032$ slit. Dates, times and pointing details are given in Table 1. Twenty spectral windows were extracted including several density sensitive spectral lines suitable for line ratio diagnostics of the electron density, N_e . Details on the dependence of the ratio of intensities of two spectral lines of the same ion can be found for example in Mariska (1992). The lines used in this study are listed in Table 2. The data were reduced using standard CDS software and the most recent calibration (version 4).

Images from the Extreme-ultraviolet Imaging Telescope (EIT/SOHO) passbands and magnetograms from the Michelson Doppler Interferometer (MDI/SOHO) were inspected to confirm the BP nature of the features: point-like or loop-like coronal structures associated to bipolar magnetic features that last for several hours (Zhang et al. 2001; Ugarte-Urra et al. 2004b). The six BPs represent different structures and sizes, including two which could be mistaken for small active regions by their size and brightness (s8605r00 and s8679r00). All the BPs had lifetimes longer than the observations periods.

Table 1. Details of the CDS observational sequences of six coronal bright points. The size of the slit (2''), the exposure time (50 seconds), the FOV (122'' \times 119'') and the extracted spectral windows are the same for all the datasets.

| Raster | Study | Date | Starting time | Coordinates | BP |
|----------|-------------|------------|---------------|----------------|-----|
| s8604r00 | TEDE22N/v13 | 1997/07/31 | 17:08 UT | -152'', -74'' | (1) |
| s8605r00 | TEDE22N/v13 | 1997/07/31 | 18:05 UT | -295'', +29'' | (2) |
| s8679r00 | TEDE22N/v13 | 1997/08/04 | 16:44 UT | -12'', -600'' | (3) |
| s8681r00 | TEDE22N/v13 | 1997/08/04 | 18:41 UT | +24'', +267'' | (4) |
| s8687r00 | TEDE22N/v13 | 1997/08/05 | 15:01 UT | +282'', -192'' | (5) |
| s8688r00 | TEDE22N/v13 | 1997/08/05 | 15:59 UT | +146'', -103'' | (6) |

Table 2. Electron density values in logarithmic scale ($\log N_e/\text{cm}^{-3}$) for selected areas in the core of six BPs observed with CDS obtained using CHIANTI (Young et al. 2003). Results include the size of the selected areas, minimum and maximum values for individual pixels (2'' \times 1'':68) within the area, as well as N_e values obtained from the averaged intensities of the region, with and without background subtraction. The wavelength values are the observed ones given by Brooks et al. (1999), ^{bl} indicates the presence of an unresolved blend, [↑] or [↓] indicate that the error is over or below the density sensitivity, while ^{NC} labels electron density values obtained after using new atomic calculations from the Iron Project for Fe xii (see text for details).

| BP | Area's size | Ion | Ratio | $\log N_e/\text{cm}^{-3}$ | | | | |
|-----|-------------------|---------|---------------|--|--|---|--|---|
| | | | | Individual pixels | | Average | | |
| | | | | Min. | Max. | Subtr. | No Subtr. | |
| (1) | 6'' \times 7'' | Fe xiv | 353.79/334.17 | - | - | - | ^{bl} 9.43 ^{+0.30} _{-0.30} | |
| | | Fe xiii | 359.78/348.15 | - | - | - | 9.56 ^{+1.67} _{-1.00} | |
| | | Fe xii | 364.47/338.26 | - | - | - | 10.20 ^{+0.26} _{-0.21} | |
| | | Si x | 356.04/347.40 | 9.16 ^{+0.72} _{-0.55} | 9.42 ^{+1.71} _{-0.53} | 9.33 ^{+0.18} _{-0.17} | 9.26 ^{+0.15} _{-0.14} | NC 9.90 ^{+0.32} _{-0.28} |
| (2) | 8'' \times 10'' | Fe xiv | 353.79/334.17 | - | - | - | ^{bl} 9.29 ^{+0.16} _{-0.17} | |
| | | Fe xiii | 359.78/348.15 | - | - | - | 9.60 [↓] | |
| | | Fe xii | 364.47/338.26 | 9.71 ^{+1.30} _{-0.60} | 10.20 [↑] _{-1.09} | 9.99 ^{+0.17} _{-0.15} | 9.95 ^{+0.16} _{-0.14} | NC 9.57 ^{+0.21} _{-0.19} |
| | | Si x | 356.04/347.40 | 8.82 ^{+0.34} _{-0.44} | 9.31 ^{+0.73} _{-0.47} | 9.16 ^{+0.10} _{-0.09} | 9.12 ^{+0.09} _{-0.08} | |
| (3) | 12'' \times 7'' | Fe xiv | 353.79/334.17 | - | - | - | ^{bl} 9.50 ^{+0.04} _{-0.04} | |
| | | Fe xiii | 359.78/348.15 | - | - | - | - | |
| | | Fe xii | 364.47/338.26 | 9.97 [↑] _{-1.6} | 10.35 [↑] _{-1.16} | 10.16 ^{+0.16} _{-0.15} | 10.13 ^{+0.14} _{-0.16} | NC 9.80 ^{+0.20} _{-0.18} |
| | | Si x | 356.04/347.40 | 9.25 ^{+0.40} _{-0.34} | 10.63 [↑] _{-1.33} | 9.23 [↑] _{-0.82} | 9.17 ^{+1.18} _{-0.77} | |
| (4) | 6'' \times 5'' | Fe xiv | 353.79/334.17 | - | - | - | ^{bl} 9.40 ^{+0.18} _{-0.23} | |
| | | Fe xiii | 359.78/348.15 | - | - | - | 9.83 ^{+0.30} _{-0.33} | |
| | | Fe xii | 364.47/338.26 | 9.94 [↑] _{-0.75} | 10.22 [↑] _{-1.09} | 10.00 ^{+0.44} _{-0.32} | 9.87 ^{+0.39} _{-0.30} | NC 9.46 ^{+0.51} _{-0.40} |
| | | Si x | 356.04/347.40 | 9.24 [↑] _{-0.77} | 9.80 [↑] _{-1.03} | 9.35 ^{+1.3} _{-0.56} | 9.12 ^{+0.44} _{-0.40} | |
| (5) | 6'' \times 7'' | Fe xiv | 353.79/334.17 | - | - | - | ^{bl} 9.21 ^{+0.23} _{-0.37} | |
| | | Fe xiii | 359.78/348.15 | - | - | - | 9.90 ^{+1.75} _{-0.37} | |
| | | Fe xii | 364.47/338.26 | 10.82 [↑] _{-1.27} | 9.70 [↑] _{-0.78} | 9.60 [↑] _{-1.01} | 9.63 [↑] _{-1.07} | NC 9.14 ^{+0.63} _{-1.21} |
| | | Si x | 356.04/347.40 | 8.99 ^{+0.39} _{-0.43} | 9.29 [↓] | 9.18 ^{+0.14} _{-0.14} | 9.12 ^{+0.12} _{-0.12} | |
| (6) | 6'' \times 7'' | Fe xiv | 353.79/334.17 | - | - | - | ^{bl} 9.20 ^{+0.33} _{-0.83} | |
| | | Fe xiii | 359.78/348.15 | - | - | - | 9.43 ^{+0.43} _{-0.46} | |
| | | Fe xii | 364.47/338.26 | - | - | - | 9.69 ^{+0.58} _{-0.39} | NC 9.22 ^{+0.76} _{-0.47} |
| | | Si x | 356.04/347.40 | 8.90 ^{+0.65} _{-0.98} | 9.39 [↑] _{-1.29} | 9.15 ^{+0.22} _{-0.20} | 8.97 ^{+0.13} _{-0.13} | |

None of them were classified as an active region in the National Oceanic and Atmospheric Administration NOAA catalog. It has to be noted here that the distinction in the literature between a small active region and an ephemeral region is arbitrary (Schrijver & Zwaan 2000, page 114). BPs can be both a result of the photospheric emergence of new magnetic flux (ephemeral regions) or, the most likely, cancellation of pre-existing magnetic features (Webb et al. 1993). Therefore, the differences between a large BP and a small active region is not well defined and can affect the results of automatized identification procedures (Sattarov et al. 2002). From the

results of this study, it appears that in terms of core electron densities there are similarities between both structures.

3. Results and discussion

Table 2 shows the electron density values obtained for the six BPs using four different line ratios of ions with temperatures ranging between 1.3–2.0 \times 10⁶ K. CHIANTI (Young et al. 2003) was used to generate the electron density sensitive curves for all the ions considered in the table. For Fe xii we also considered new atomic calculations (see discussion later).

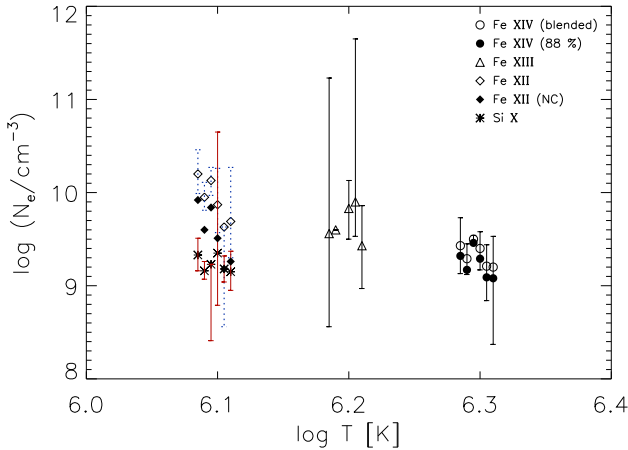


Fig. 1. Electron density as a function of formation temperature for the six BPs. All datapoints with the same symbol should be plotted at the same temperature position, but have been spread for clarity. The Fe XII (NC) are these using the new atomic data of Storey et al. (2005), while Fe XII (open diamonds) are from CHIANTI (Young et al. 2003).

The electron density values were obtained for the pixels inside a selected area in the core of each BP. The size of these areas are indicated in the second column of the table. The fourth and fifth column give the minimum and maximum N_e values of individual pixels ($2'' \times 1''.68$), for those spectral lines with sufficient signal to noise to permit the Gaussian fit of the spectral profiles. Acknowledging that the recorded emission coming from the BP direction is a superposition of the BP's emission plus the emission from plasma in the line-of-sight, the average intensity of a $22'' \times 18''$ neighbouring and quiet area was subtracted for every image and every line, as an estimate of that contamination. As the uncertainties are large for individual pixels, the ratio from the averaged intensities of the BPs' core areas was also calculated, producing the N_e values given in columns 6 & 7. These are respectively the values obtained after and before background subtraction. The differences between the two results are systematic, with larger N_e values after subtracting the faint and less dense background (which smooths the results with no subtraction). However, they are indistinguishable within the uncertainties. This justifies the use of the non-subtracted N_e values of the hottest lines as a good estimate, when the subtraction is not feasible.

The hottest lines used in the diagnostics (Fe XIV, Fe XIII) are the weakest in the dataset. Even though the BPs show a contrast with respect to the surrounding background corona, either the counts are too low to retrieve a proper Gaussian fit for individual pixels and/or the averaged background, or after fitted, the errors in the intensity are too large to produce a meaningful estimate. The error bars given in Table 2 are the result of the propagation of the errors coming from the fit.

Figure 1 shows the N_e background subtracted values for Si X and the values with no subtraction for Fe XII, Fe XIII and Fe XIV as a function of the formation temperature of the ion in ionization equilibrium. All data-points with the same symbol should be at the same temperature position, but have been spread for clarity. Data-points with no error bars are those with

large uncertainties reaching the limits of the density sensitivity of the ratio. The first thing to notice from the plot is the systematic higher values obtained with Fe XII (open diamonds) compared to Si X (asterisks), both with the same formation temperature. Previous works have noted the discrepancy (e.g. Mason et al. 1999; Gallagher et al. 2001) between the densities obtained from Fe XII and those from other ions formed at similar temperature. This could be due to three reasons: in first place and following the argument given by Doschek (1984), if the plasma is highly inhomogeneous, similar density diagnostics can provide different density results due to the different dependence with density of the lines, which produces a different weighting of the emission in the averaging. A second possibility is that the Fe XII collisional rates are inaccurate or thirdly that un-accounted blends are present (e.g. Binello et al. 2001).

New Fe XII collision strengths have recently been calculated by Storey et al. (2005). These new calculations, done as part of the Iron Project, use the *R*-matrix approach and represent a significant improvement over all previous calculations, that either had an inaccurate target or underestimated the contribution from resonances to the collision strengths. As shown in Storey et al., the new data appear to solve the long-standing problem of the high electron densities previously obtained with Fe XII line ratios, at least in quiet Sun spectra. In active region (hereafter AR) data, the possibility that the Fe XII 338.3 Å line was slightly blended was left open. The Fe XII ion model has been completed with the transition probabilities calculated by Del Zanna & Mason (2005). The Fe XII electron density values from the new calculations (NC) are shown with filled diamonds in Figure 1. The values are notably below the original ones, a factor of two or more less, and some of them come into agreement with the Si X ones, although only the ones with larger uncertainties. The best constrained values are still higher than those of Si X, suggesting that some further improvement (e.g. a blending of the Fe XII 338.3 Å) might be needed. A 10% contribution from a blend would be enough to make the error bars overlap. In fact, some of the line profiles indicate the possible presence of a blend at 338.1 Å.

The Si X N_e values are very consistent for all the BPs and what is more interesting, they are in the range of values presented by Landi & Landini (1998, $\log N_e = 9.0 \pm 0.4$), Mason et al. (1999, $\log N_e \approx 8.9 - 9.2$) and Gallagher et al. (2001, $\log N_e = 9.1 \pm 0.2$) in their study of AR using the same ion, and slightly larger than the quiet Sun densities given by Landi & Landini (1998). The average density of the four BPs with a better constrained uncertainty is $\log N_e = 9.21 \pm 0.17$.

The Fe XIII 359.64 Å line presents a strong blend with the Ne V 359.38 Å, which could be unblended with a double Gaussian, but which introduces large uncertainties in the N_e results. Despite that fact, the density seems to indicate an increase with respect to the Si X values, similar to the density increase showed by Mason et al. (1999) for two active regions. Our Fe XIII N_e measurements, however, are larger than theirs, which are similar to those presented by Gallagher et al. (2001) and one of Brosius et al. (1996) ARs, with $\log N_e \approx 9.1$, but are closer to the results obtained by Young et al. (1998) and the other Brosius et al. (1996) AR, in the range 9.3 – 9.6. There seems to be a variety of measurements for different active re-

gions that could be due to intrinsic properties, but also to the selection of the area where the emission is averaged. What seems clear is that the electron densities found in these BPs are more consistent with active region plasma than with quiet Sun plasma. A comparison between quiet Sun and active region values can be found for *e.g.* in Brosius et al. (1996).

The Fe XIV 353.84 Å line is blended with an Al VII 353.78 Å which could not be unblended in the fit. The results without removing the blend are the open circles in Figure 1. Having postulated that the plasma has similarities with an active region plasma, the density values were also determined assuming that the Al VII 353.78 Å intensity contributes 12% to the blend, an estimate obtained from a CHIANTI theoretical spectrum using an active region differential emission measure (Vernazza & Reeves 1978). The results are shown with filled circles. The difference is minimal and within the error bars. A high resolution spectrum (50–80 mÅ) of an active region obtained with the *Solar EUV Rocket Telescope and Spectrograph* (SERTS; Thomas & Neupert 1994) indicates a contribution of only 3%. With these considerations, the Fe XIV density values seem to be much lower than the ones found in active regions by the previous cited works. It is difficult from this plot with only three useful ratios and large uncertainties in the case of Fe XIII to conclude if the increase for that ion is real. A constant N_e scenario can not be ruled out. A density sensitive ratio at cooler temperatures is present in the dataset, Mg VII 367.67/319.02 ($T_e = 6.3 \times 10^5$ K), but the 319.02 Å line is a weak line blended with a Ni XV line at 319.06 Å (Young et al. 1998), and reliable results could not be obtained. Refined measurements will be needed to confirm the trend and extend it to other temperature ranges.

4. Conclusions

Electron density measurements of six coronal bright points have been obtained using line ratio diagnostics of four ions in the temperature range $1.3\text{--}2.0 \times 10^6$ K. The results suggest that BP plasma has more similarities to active region plasma than to quiet Sun plasma. Nevertheless, they do not show the exact same behaviour: the increase of electron density at temperatures over $\log T_e \sim 6.2$, observed in the core of active regions (Mason et al. 1999; Gallagher et al. 2001), has not been detected in BPs. More observations by new missions, like the forthcoming Solar-B/EIS, with improved spatial resolution and sensitivity should be able to study the constituent loops of BPs and determine if their characteristics are similar to active region loops. So far, TRACE studies on the BPs' small scale evolution suggest that BPs' loops might be more dynamic, having shorter lifetimes (Brown et al. 2001; Ugarte-Urra 2004).

The electron density measurements for Si X and Fe XII, two ions with the same formation temperature, give inconsistent results. It has been argued over the years that this arises from inaccurate atomic calculations. Therefore, new collision strengths (Storey et al. 2005) have been used and the electron densities determined. The new results, although in better agreement decreasing up to 68% the initial densities, are still higher in some instances than the Si X ones. New measurements in other solar structures with a better constriction of the volumet-

ric properties seem necessary to rule out the influence of other factors and confirm whether there is still an inconsistency between the ions, or whether it is due to line blending problems.

Acknowledgements. Research at Armagh Observatory is grant-aided by the N. Ireland Dept. of Culture, Arts and Leisure. This work was supported by a PRTLI research grant for Grid-enabled Computational Physics of Natural Phenomena (Cosmogrid). CDS, EIT and MDI are instruments onboard SOHO. SOHO is a project of international cooperation between ESA and NASA. CHIANTI is a collaborative project involving the NRL (USA), RAL (UK), and the Universities of Florence (Italy) and Cambridge (UK).

References

- Binello, A. M., Landi, E., Mason, H. E., Storey, P. J., & Brosius, J. W. 2001, *A&A*, 370, 1071
- Brooks, D. H., Fischbacher, G. A., Fludra, A., et al. 1999, *A&A*, 347, 277
- Brosius, J. W., Davila, J. M., Thomas, R. J., & Monsignori-Fossi, B. C. 1996, *ApJS*, 106, 143
- Brown, D. S., Parnell, C. E., Deluca, E. E., Golub, L., & McMullen, R. A. 2001, *Sol. Phys.*, 201, 305
- Del Zanna, G., Bromage, B. J. I., & Mason, H. E. 2003, *A&A*, 398, 743
- Del Zanna, G. & Mason, H. 2005, *A&A*, in press
- Doschek, G. A. 1984, *ApJ*, 279, 446
- Gallagher, P. T., Phillips, K. J. H., Lee, J., Keenan, F. P., & Pinfield, D. J. 2001, *ApJ*, 558, 411
- Landi, E. & Landini, M. 1998, *A&A*, 340, 265
- Mariska, J. T. 1992, *The solar transition region* (Cambridge Astrophysics Series, New York: Cambridge University Press, —c1992)
- Mason, H. E., Landi, E., Pike, C. D., & Young, P. R. 1999, *Sol. Phys.*, 189, 129
- McIntosh, S. W. & Gurman, J. B. 2004, in *ESA SP-575: SOHO 15 Coronal Heating*, 235
- Sattarov, I., Pevtsov, A. A., Hojaev, A. S., & Sherdonov, C. T. 2002, *ApJ*, 564, 1042
- Schrijver, C. J. & Zwaan, C. 2000, *Solar and stellar magnetic activity* (New York : Cambridge University Press, 2000. Cambridge astrophysics series ; 34)
- Storey, P., Del Zanna, G., Mason, H., & Zeippen, C. 2005, *A&A*, in press
- Thomas, R. J. & Neupert, W. M. 1994, *ApJS*, 91, 461
- Ugarte-Urra, I. 2004, Ph.D. Thesis, Queen's University, Belfast.
- Ugarte-Urra, I., Doyle, J. G., Madjarska, M. S., & O'Shea, E. 2004a, *A&A*, 418, 313
- Ugarte-Urra, I., Doyle, J. G., Nakariakov, V. M., & Foley, C. R. 2004b, *A&A*, 425, 1083
- Vernazza, J. E. & Reeves, E. M. 1978, *ApJS*, 37, 485
- Webb, D. F., Martin, S. F., Moses, D., & Harvey, J. W. 1993, *Sol. Phys.*, 144, 15
- Young, P. R., Del Zanna, G., Landi, E., et al. 2003, *ApJS*, 144, 135
- Young, P. R., Landi, E., & Thomas, R. J. 1998, *A&A*, 329, 291
- Zhang, J., Kundu, M. R., & White, S. M. 2001, *Sol. Phys.*, 198, 347